IMPLICIT IMPLEMENTATION OF CHABOCHE CYCLIC PLASTICITY MODEL

LOPES, J. P.
MALCHER, L.
jhonatan_plopes@hotmail.com
malcher@unb.br
University of Brasilia, Faculty of Engineering, Mechanical Engineering Department
Darcy Ribeiro Campus, SG9 Building, Brasília – Distrito Federal – Brazil

Abstract. *This paper seeks the implicit implementation of the Chaboche model, utilizing the von Mises' yield function. Initially, the von Mises' and Chaboche kinematic hardening model is developed, by formulating the necessary constitutive relations. Then, the numerical model necessary to the solution of the constitutive relations is developed, utilizing the Chaboche law with 3 terms and Euler's discretization. The implementation results are presented, referring to Chaboche law with two non-linear terms and one linear term and Armstrong-Frederick law (Chaboche with one non-linear term). Steels 304 and S460N were utilized, being subjected to uniaxial traction-compression, uniaxial shear, multiaxial proportional and multiaxial non-proportional loading trajectories. The results are compared among themselves and with experimental data.*
Keywords: *Cyclic Plasticity, Kinematic Hardening, Implicit Implementation*

1 INTRODUCTION

The importance of knowing the elastoplastic behavior of materials is of vital importance, especially in the design of products and processes. In stamping, cutting and folding processes, for instance, the material is being loaded mainly in the plastic regime. Thus, knowing the elastoplastic behavior allows us to design avoiding excessive stresses and deformations that could damage the material, causing the appearance of defects such as cracks, for example.

Cyclic plasticity is directly related to fatigue failure. In mechanical components subjected to variable loads, the fatigue phenomenon stands out among the failure mechanisms, being characterized by the fracture of the material, due to the growth of microcracks during alternating cycles of loading and unloading. Its consequences can be catastrophic, such as the explosion in flight of the Comet aircrafts in 1954, caused by the fuselage fracture due to fatigue at the ends of the windows; and the derailment of the German high speed train ICE in 1998, due to fatigue on its wheels, killing over a hundred people. Because of its complexity, fatigue has been the subject of study of the scientific and industrial community since the nineteenth century, and its quantification is still a challenge.

In order to obtain a reliable mechanical design, the fatigue models require the loading history including mean stresses and stress amplitudes to which the engineering components are subjected. In some cases, mechanical testing can be used to obtain a safe design. However, for complex geometries and loadings, the determination of those parameters is not trivial, and depends on the use of complex models. Therefore, in those cases it is necessary to formulate and use mathematical/numerical models to determine the loading history.

For alternating loadings in plastic regime, the cyclic plasticity models of Armstrong & Frederick (1966) and Chaboche (1986) stand out, due to their description of the Baushinger Effect which takes place when the material is subjected to cyclic loading.

Therefore, the objective of this paper is to implement the mathematical/numerical cyclic plasticity model of Chaboche with von Mises' yield function. A 3D model will be developed to implicitly integrate the evolution relations.

2 MATHEMATICAL RELATIONS AND NUMERICAL INTEGRATION

The von Mises' yield function is described by the Eq. 1, where $\boldsymbol{\eta}$ is the relative stress tensor and σ_{y0} is the initial yield strength (Souza Neto et. al., 2008).

$$\phi = \sqrt{\frac{3}{2}\boldsymbol{\eta}:\boldsymbol{\eta}} - \sigma_{y0} \tag{1}$$

The relative stress tensor is given by Eq. 2, where $\boldsymbol{s}(\boldsymbol{\sigma})$ is the stress deviator tensor and $\boldsymbol{\beta}$ the backstress tensor, which is the thermodynamical force associated with kinematic hardening and represents the translation of the yield surface in the space of stress (Souza Neto et. al., 2008).

$$\boldsymbol{\eta}(\boldsymbol{\sigma},\boldsymbol{\beta}) \equiv \boldsymbol{s}(\boldsymbol{\sigma}) - \boldsymbol{\beta} \tag{2}$$

The cyclic plastic behavior depends on the description of the backstress' evolution. According to Chaboche (1986), when utilizing 3 non-linear terms, $\dot{\boldsymbol{\beta}}$ is given as:

$$\dot{\boldsymbol{\beta}} = \sum_{i=1}^{3}\left(\frac{2}{3}H_i^k\dot{\boldsymbol{\varepsilon}^{p}} - \dot{\bar{\varepsilon}}^p b_i \boldsymbol{\beta}_i\right) \tag{3}$$

where H_i^k and b_i are material parameters, $\dot{\boldsymbol{\varepsilon}^{p}}$ is the rate of plastic strain tensor and $\dot{\bar{\varepsilon}}^p$ the accumulated plastic strain. Generally, the use of 2 non-linear terms ($2/3\, H_i^k\dot{\boldsymbol{\varepsilon}^{p}} - \dot{\bar{\varepsilon}}^p b_i \boldsymbol{\beta}_i$) and 1 linear term ($2/3\, H_i^k\dot{\boldsymbol{\varepsilon}^{p}}$) gives good results when compared to experimental data (Chaboche, 1986). The use of 3 non-linear terms in the model formulation is for convenience.

The necessary relations for the von Mises/Chaboche elastoplastic model are given in the Table 1.

Table 1. Elastoplastic model with von Mises' yield function and Chaboche kinematic hardening.

i)	Additive decomposition of the strain tensor $\boldsymbol{\varepsilon} = \boldsymbol{\varepsilon}^e + \boldsymbol{\varepsilon}^p$
ii)	Hooke's law $\boldsymbol{\sigma} = \mathbb{D}^e : \boldsymbol{\varepsilon}^e$
iii)	Yield function $\phi = \sqrt{\frac{3}{2}\boldsymbol{\eta}:\boldsymbol{\eta}} - \sigma_{y0}$ $\boldsymbol{\eta} = \boldsymbol{s} - \boldsymbol{\beta}$
iv)	Plastic flow rule $\dot{\boldsymbol{\varepsilon}}^p = \dot{\gamma}\frac{3\boldsymbol{\eta}}{2\bar{q}}$ Hardening law and accumulated plastic strain rate $\dot{\bar{\varepsilon}}^p = \dot{\gamma}$ $\dot{\boldsymbol{\beta}} = \dot{\gamma}\sum_{i=1}^{3}\left(H_i^k\frac{\boldsymbol{\eta}}{\bar{q}} - b_i\boldsymbol{\beta}_i\right)$
v)	Loading/unloading criterion $\dot{\gamma} \geq 0, \quad \phi \leq 0, \quad \dot{\gamma}\phi = 0$

Euler's discretization is then applied. Developing the constitutive equations to the correction of the trial state, it is found a non-linear system of equations composed by the following variables: $\boldsymbol{S}_{n+1}$, $\boldsymbol{\beta}_{n+1}^1$, $\boldsymbol{\beta}_{n+1}^2$, $\boldsymbol{\beta}_{n+1}^3$, $\bar{\boldsymbol{\varepsilon}}_{n+1}^p$ and $\Delta\gamma$, where $\Delta\gamma$ is the plastic multiplier. Equation 4 represents the system of equations in the residual form, which is solved implicitly using Newton-Raphson method.

$$\begin{aligned}
R_{\boldsymbol{S}_{n+1}} &= \boldsymbol{S}_{n+1} - \boldsymbol{S}_{n+1}^{trial} + 2G\Delta\gamma\boldsymbol{N}_{n+1} \\
R_{\bar{\boldsymbol{\varepsilon}}_{n+1}^p} &= \bar{\varepsilon}_{n+1}^p - \bar{\varepsilon}_n^p - \Delta\gamma \\
R_{\Delta\gamma} &= \sqrt{\tfrac{3}{2}\boldsymbol{\eta}_{n+1}:\boldsymbol{\eta}_{n+1}} - \sigma_{y0} \\
R_{\boldsymbol{\beta}_{n+1}^1} &= \boldsymbol{\beta}_{n+1}^1 - \boldsymbol{\beta}_n^1 - \Delta\gamma\left(\tfrac{2H_1^k}{3}\boldsymbol{N}_{n+1} - b_1\boldsymbol{\beta}_{n+1}^1\right) \\
R_{\boldsymbol{\beta}_{n+1}^2} &= \boldsymbol{\beta}_{n+1}^2 - \boldsymbol{\beta}_n^2 - \Delta\gamma\left(\tfrac{2H_2^k}{3}\boldsymbol{N}_{n+1} - b_2\boldsymbol{\beta}_{n+1}^2\right) \\
R_{\boldsymbol{\beta}_{n+1}^3} &= \boldsymbol{\beta}_{n+1}^3 - \boldsymbol{\beta}_n^3 - \Delta\gamma\left(\tfrac{2H_3^k}{3}\boldsymbol{N}_{n+1} - b_3\boldsymbol{\beta}_{n+1}^3\right)
\end{aligned} \tag{4}$$

3 MATERIAL PARAMETERS IDENTIFICATION

The numerical model developed was implemented in order to compare the Chaboche and Armstrong-Frederick laws with experimental data. To do so, the material parameters H_2^k, H_3^k, b_2 and b_3 were set as zero, which gives the Armstrong-Frederick backstress evolution law described in Eq. 5.

$$\dot{\boldsymbol{\beta}} = \frac{2}{3} H_1^k \dot{\boldsymbol{\varepsilon}}^{\boldsymbol{p}} - \dot{\gamma} b_1 \boldsymbol{\beta}_1 \tag{5}$$

Two non-linear terms and one linear term were utilized in Chaboche implementation, as recommended (Chaboche, 1986), which gives the backstress evolution described in Eq. 6. In this case, the parameter b_3 was set as zero.

$$\dot{\boldsymbol{\beta}} = \frac{2}{3} H_1^k \dot{\boldsymbol{\varepsilon}}^{\boldsymbol{p}} - \dot{\gamma} b_1 \boldsymbol{\beta}_1 + \frac{2}{3} H_2^k \dot{\boldsymbol{\varepsilon}}^{\boldsymbol{p}} - \dot{\gamma} b_2 \boldsymbol{\beta}_2 + \frac{2}{3} H_3^k \dot{\boldsymbol{\varepsilon}}^{\boldsymbol{p}} \tag{6}$$

The material parameters were identified by fitting Eq. 7 (Chaboche, 1986) to the Ramberg-Osgood stress-strain amplitude curve obtained from Itoh (2001) for 304 steel and Jiang et al. (2007) for S460N steel. The results for the Armstrong-Frederick and Chaboche models are presented in Tables 2 and 3 respectively.

$$\frac{\Delta\sigma}{2} = \frac{H_1^k}{b_1} \tanh\left(b_1 \frac{\Delta\varepsilon^P}{2}\right) + \frac{H_2^k}{b_2} \tanh\left(b_2 \frac{\Delta\varepsilon^P}{2}\right) + H_3^k b_2 \frac{\Delta\varepsilon^P}{2} + \sigma_y \tag{7}$$

Table 2 – Calibration results for Armstrong-Frederick model and Ramberg-Osgood parameters to 304 and S460N steels.

Parameter	*Steel*	
	304 (Itoh, 2001)	*S460N (Jiang et al., 2007)*
H' (MPa)	2443	1115
n'	0.334	0.161
H^k(MPa)	82636	62837
b	319.5	378.6
σ_{y0} (MPa)	160.2	264.1
E (GPa)	193	209
ν	0.29	0.30

Table 3 – Calibration results for Chaboche model and Ramberg-Osgood parameters to 304 and S460N steels.

Parameter	*Steel*	
	304 (Itoh, 2001)	*S460N (Jiang et al., 2007)*
H' (MPa)	2443	1115
n'	0.334	0.161
H_1^k (MPa)	89382	38718
H_2^k (MPa)	46742	90521
H_3^k (MPa)	28087	15903
b_1	1547.4	486.0
b_2	454.2	1637.3
σ_{y0} (MPa)	118.1	264.1
E (GPa)	193	209
ν	0.29	0.30

4 NUMERICAL RESULTS

Numerical simulations were carried utilizing 304 and S460N steels for Chaboche and Armstrong-Frederick laws. The results were compared with experimental data. An academic finite elements tool was used in the simulation. Four separate loadings were analyzed (Fig. 1): uniaxial tensile-compression (A); pure uniaxial shear (B); proportional multiaxial (C); and non-proportional multiaxial with rectangular path (D). For all loads the same strain amplitudes and the same number of steps per cycle were used. The analysis was based on the stress amplitudes after stabilization.

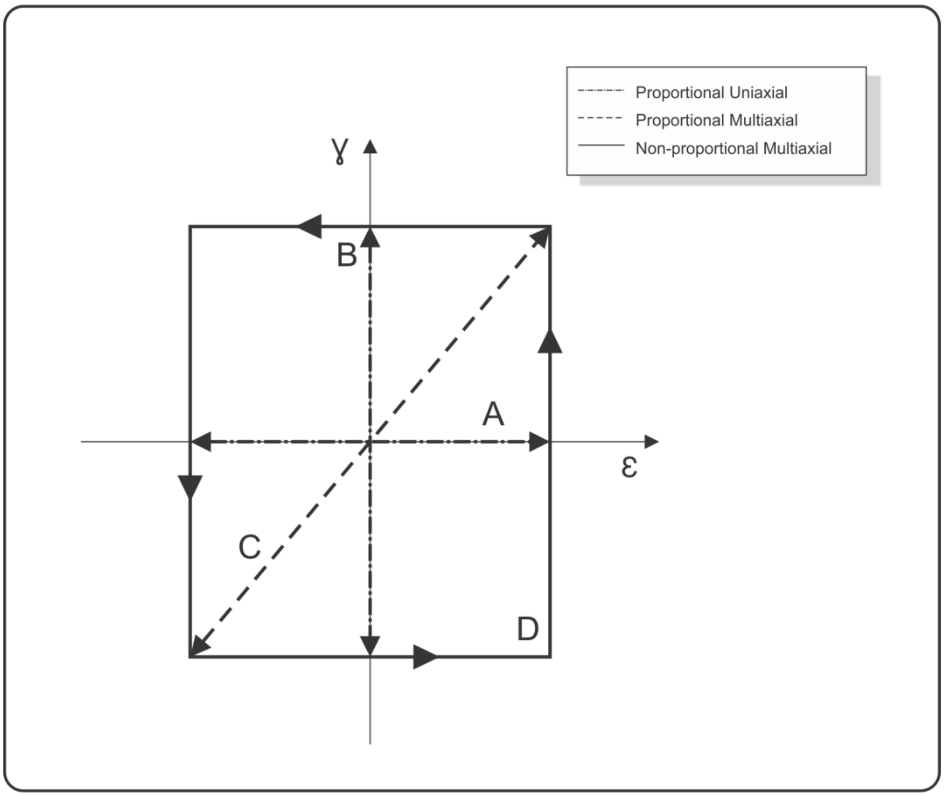

Figure 1 – Loading histories prescribed.

The prescribed strain amplitudes for each trajectory and the obtained stress results are presented in Table 4 for Armstrong-Frederick and Table 5 for Chaboche.

Figures 2 through 5 compare the Armstrong-Frederick model with Chaboche model for 304 steel, while Figs. 6 through 9 compare those two models for S460N steel.

Table 4 – Prescribed strain amplitudes and obtained numerical and experimental stress amplitudes for Armstrong-Frederick model.

Material	*Trajectory*	ε_a *(%)*	γ_a *(%)*	σ_a^{exp} *(MPa)*	τ_a^{exp} *(MPa)*	σ_a *(MPa)*	τ_a *(MPa)*
304 Steel	A	0.4	0	315	0	464	0
	B	0	0.695	-	-	0	192
	C	0.4	0.695	295	125	419	163
	D	0.4	0.695	530	278	493	212
S460N Steel	A	0.173	0	-	-	331	0
	B	0	0.3	-	-	0	189
	C	0.173	0.3	244	147	275	155
	D	0.173	0.3	362	227	334	194

Table 5 – Prescribed strain amplitudes and obtained numerical and experimental stress amplitudes for Chaboche model.

Material	*Trajectory*	ε_a *(%)*	γ_a *(%)*	σ_a^{exp} *(MPa)*	τ_a^{exp} *(MPa)*	σ_a *(MPa)*	τ_a *(MPa)*
304 Steel	A	0.4	0	315	0	428	0
	B	0	0.695	-	-	0	153
	C	0.4	0.695	295	125	376	120
	D	0.4	0.695	530	278	437	158
S460N Steel	A	0.173	0	-	-	318	0
	B	0	0.3	-	-	0	181
	C	0.173	0.3	244	147	270	150
	D	0.173	0.3	362	227	332	191

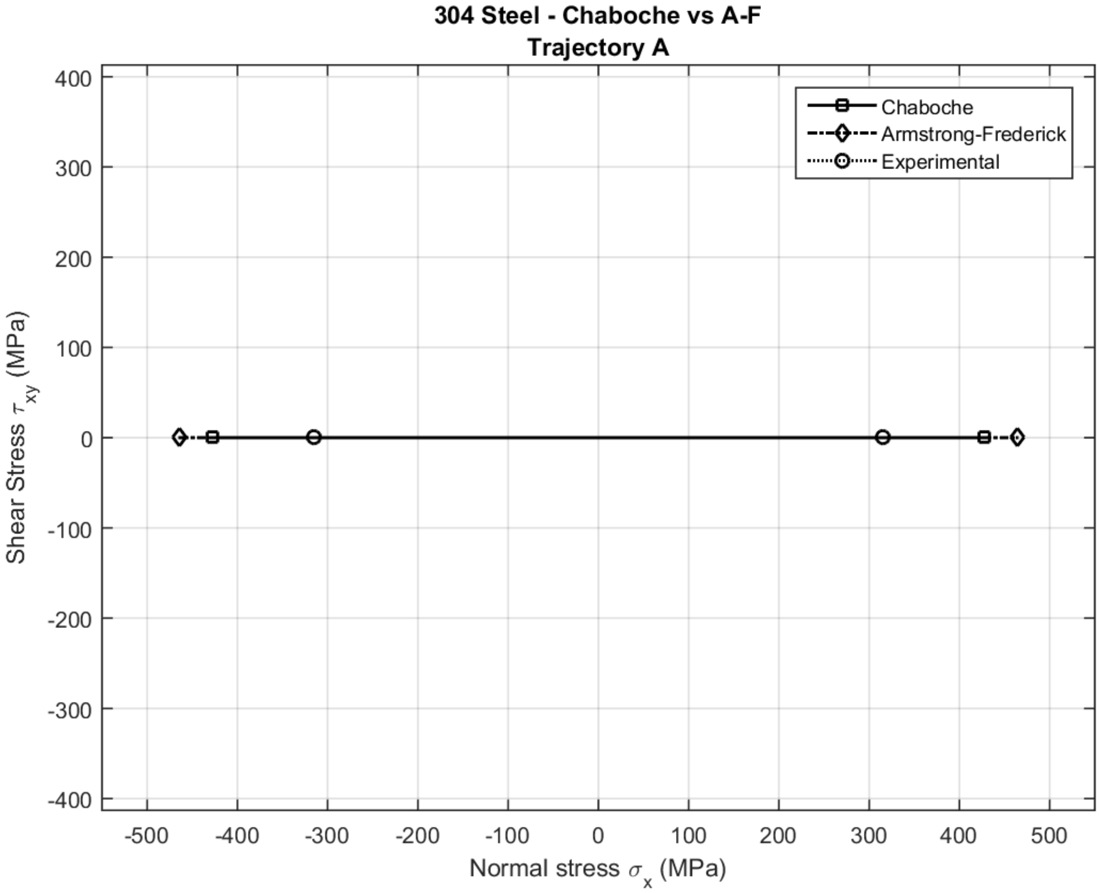

Figure 2– Comparison of stress amplitudes from uniaxial tensile-compression loading (Trajectory A) to Chaboche and Armstrong-Frederick models and experimental data (Itoh, 2001) to 304 steel, with strain amplitudes $\boldsymbol{\varepsilon_a = 0.4}$ % and $\boldsymbol{\gamma_a = 0}$ %.

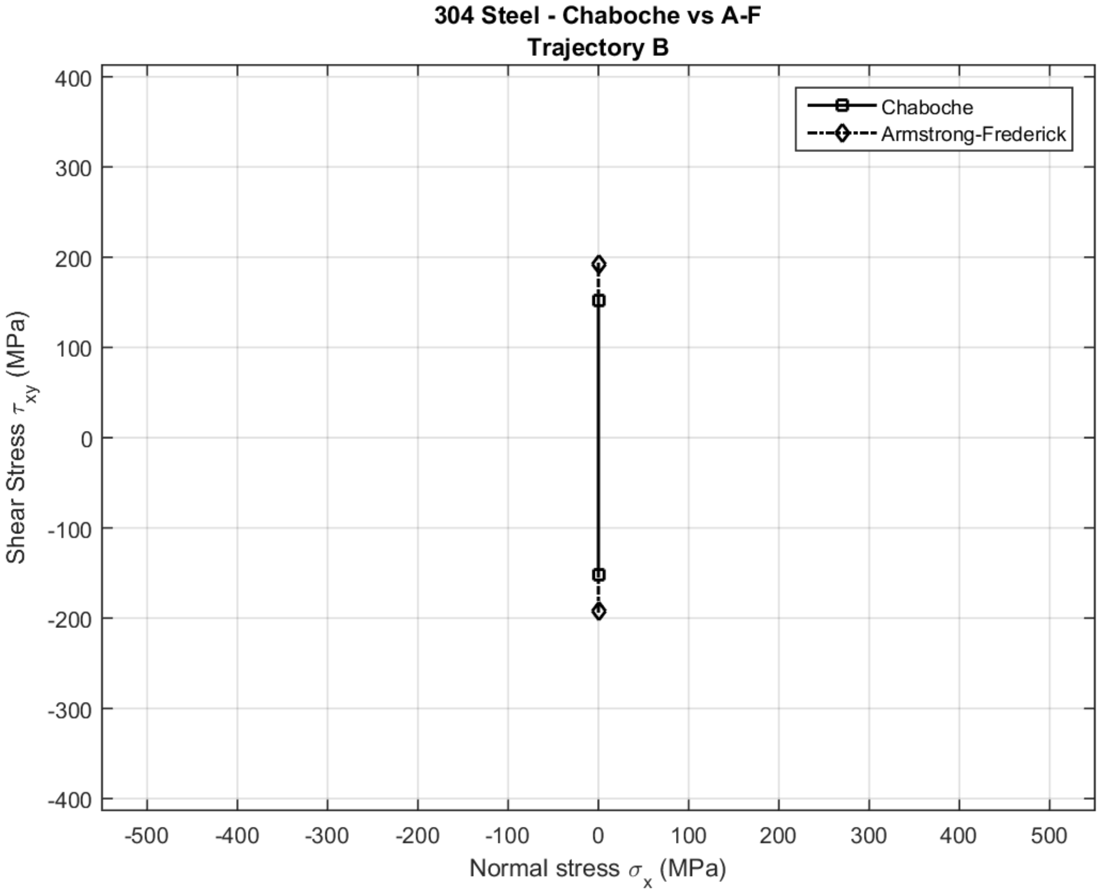

Figure 3 – Comparison of stress amplitudes from pure uniaxial shear loading (Trajectory B) to Chaboche and Armstrong-Frederick models and experimental data (Itoh, 2001) to 304 steel, with strain amplitudes $\boldsymbol{\varepsilon_a = 0}$ % and $\boldsymbol{\gamma_a = 0.695}$ %.

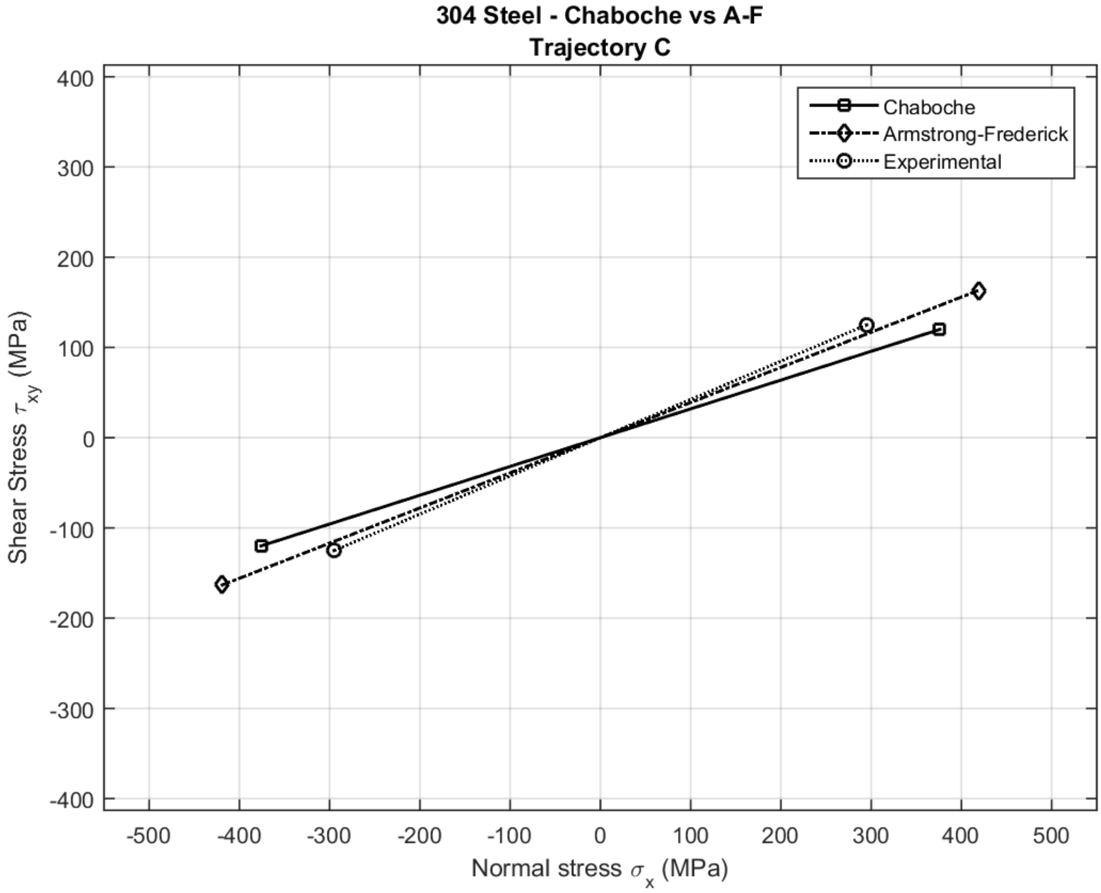

Figure 4 – Comparison of stress amplitudes from pure multiaxial proportional loading (Trajectory C) to Chaboche and Armstrong-Frederick models and experimental data (Itoh, 2001) to 304 steel, with strain amplitudes $\boldsymbol{\varepsilon_a = 0.4}$ % and $\boldsymbol{\gamma_a = 0.695}$ %.

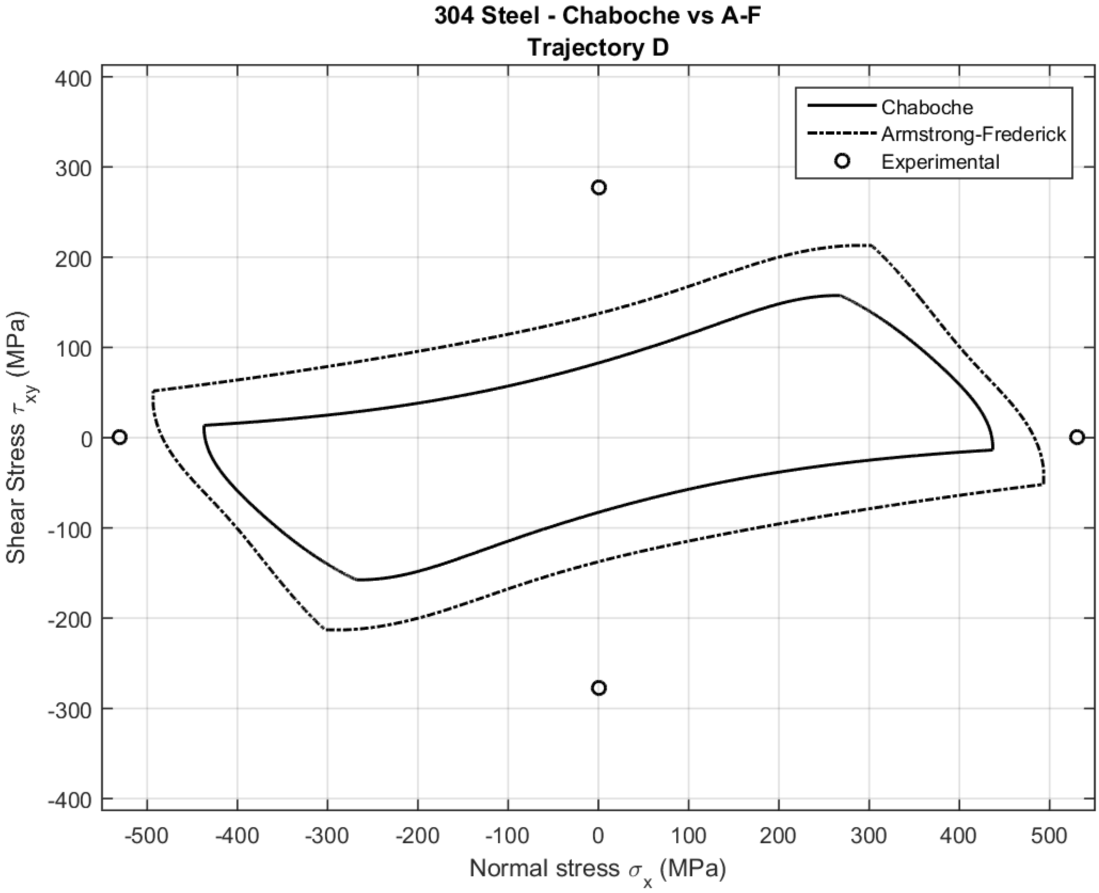

Figure 5 – Comparison of stress amplitudes from pure multiaxial non-proportional loading (Trajectory D) to Chaboche and Armstrong-Frederick models and experimental data (Itoh, 2001) to 304 steel, with strain amplitudes $\varepsilon_a = 0.4$ % and $\gamma_a = 0.695$ %.

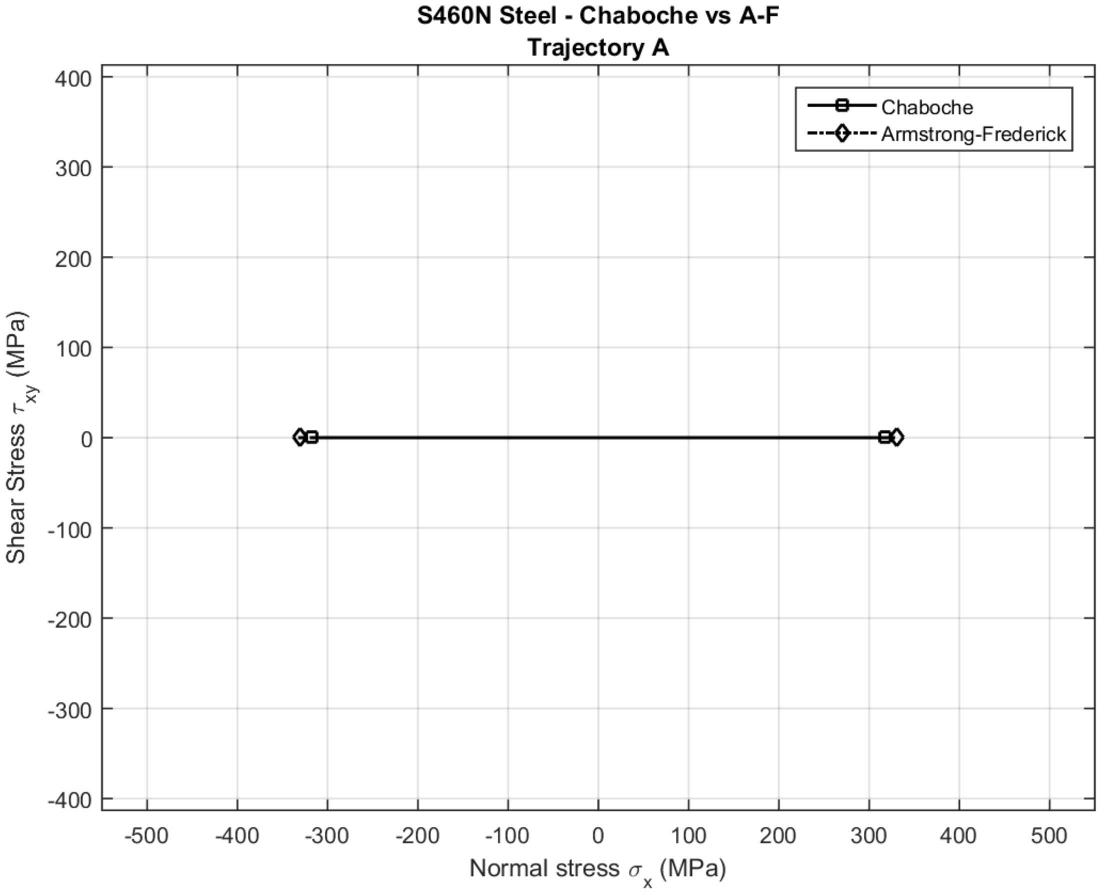

Figure 6 – Comparison of stress amplitudes from uniaxial tensile-compression loading (Trajectory A) to Chaboche and Armstrong-Frederick models and experimental data (Itoh, 2001) to S460N steel, with strain amplitudes $\boldsymbol{\varepsilon_a = 0.173}$ % and $\boldsymbol{\gamma_a = 0}$ %.

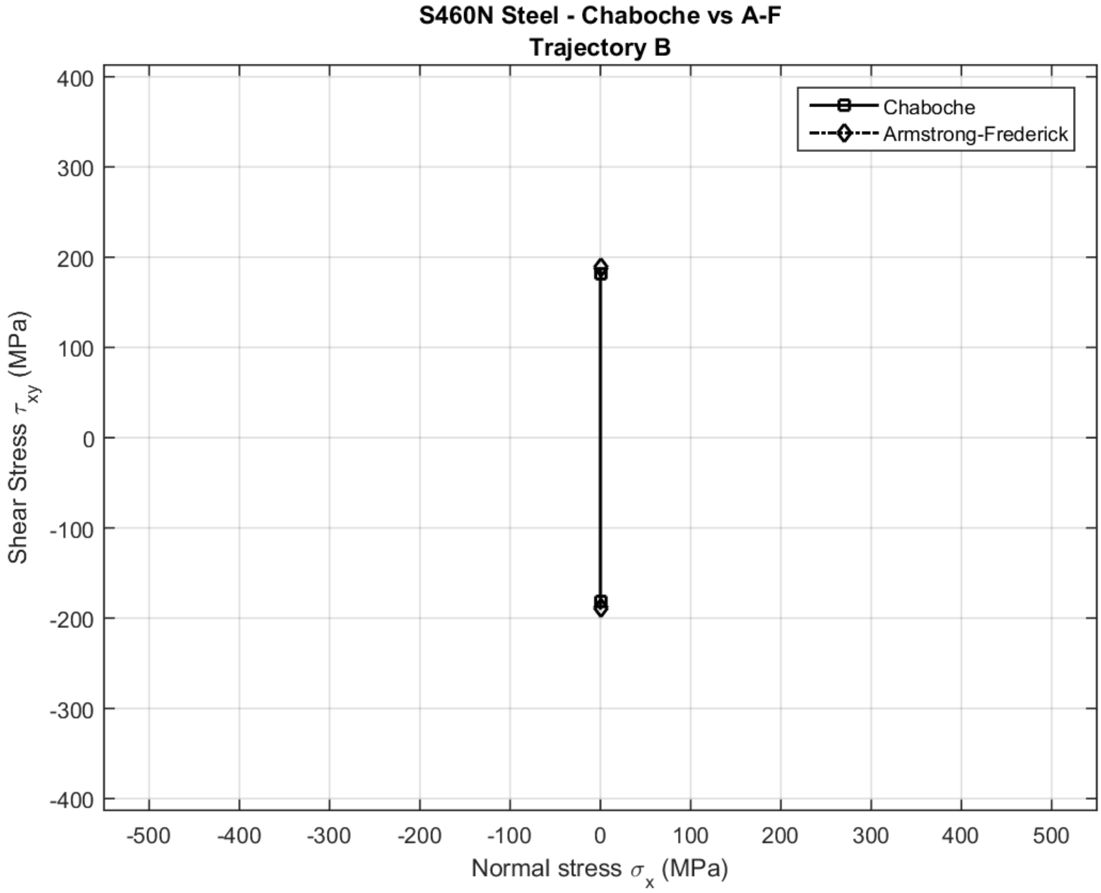

Figure 7 – Comparison of stress amplitudes from uniaxial shear loading (Trajectory B) to Chaboche and Armstrong-Frederick models and experimental data (Itoh, 2001) to S460N steel, with strain amplitudes $\boldsymbol{\varepsilon_a = 0}$ % and $\boldsymbol{\gamma_a = 0.3}$ %.

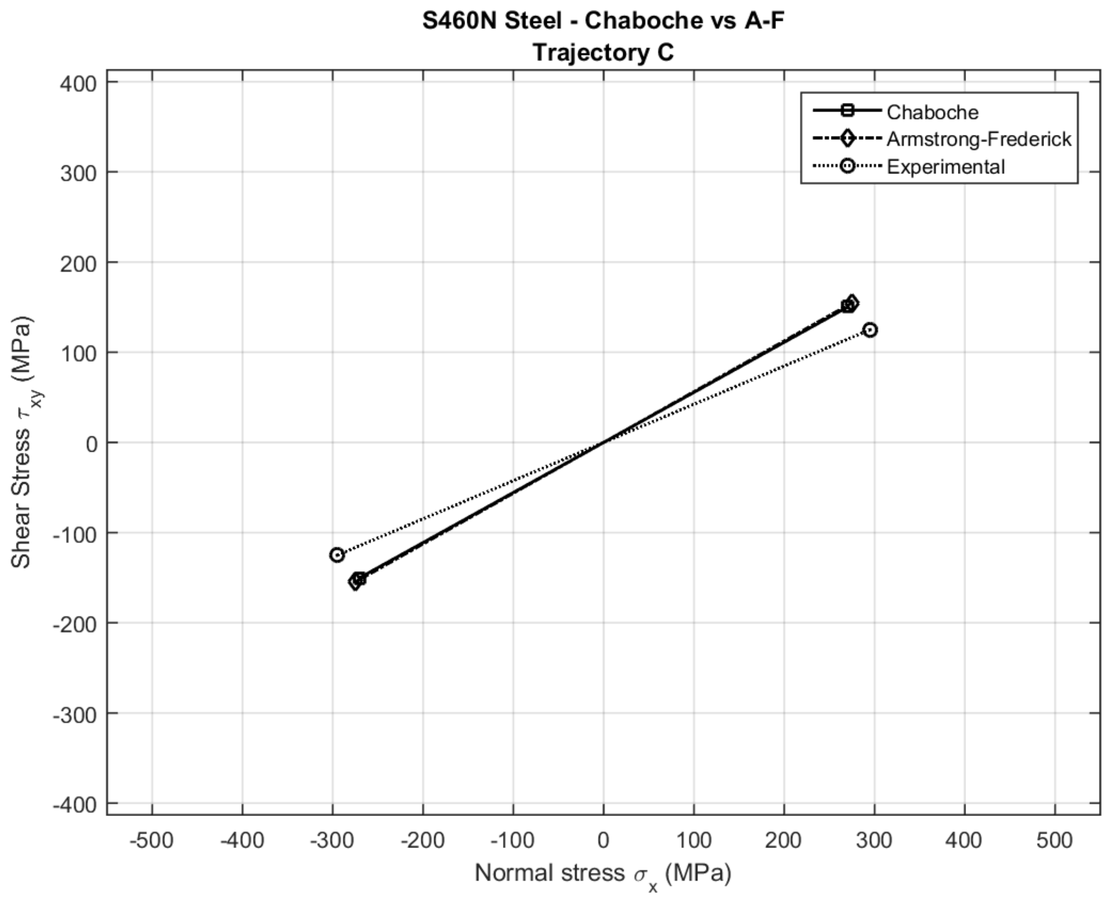

Figure 8 – Comparison of stress amplitudes from multiaxial proportional loading (Trajectory C) to Chaboche and Armstrong-Frederick models and experimental data (Itoh, 2001) to S460N steel, with strain amplitudes $\boldsymbol{\varepsilon_a = 0.173}$ % and $\boldsymbol{\gamma_a = 0.3}$ %.

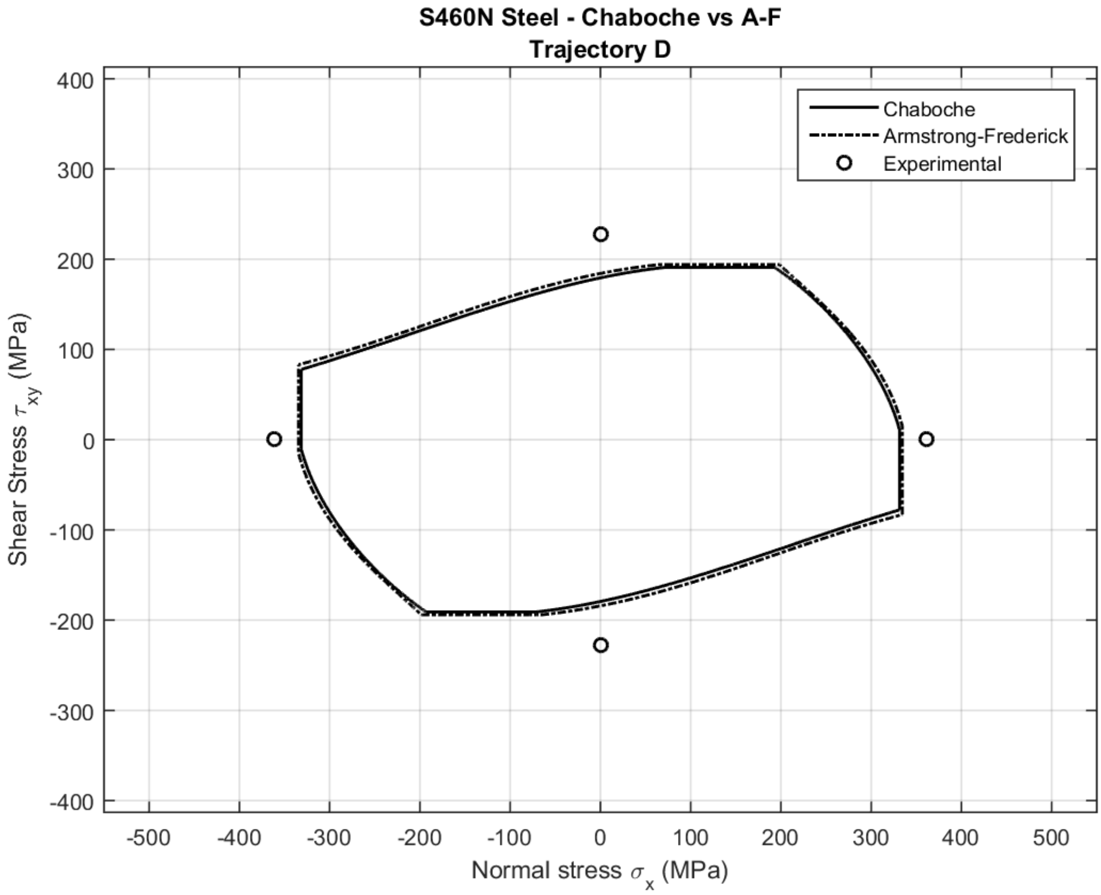

Figure 9 – Comparison of stress amplitudes from multiaxial non-proportional loading (Trajectory D) to Chaboche and Armstrong-Frederick models and experimental data (Itoh, 2001) to S460N steel, with strain amplitudes $\boldsymbol{\varepsilon_a = 0.173}$ % and $\boldsymbol{\gamma_a = 0.3}$ %.

5 CONCLUSION

From the data, it is seen that Chaboche results were closer to the experimental data and better described the materials behavior than Armstrong-Frederick model, except from trajectory D for 304 steel. For S460N steel, the results from the two models were close among each other and gave a good description of the experimental data. The maximum difference between calculated and experimental stresses is 36 MPa, corresponding to Chaboche model trajectory D. For 304 steel, the Chaboche results were closer to the experimental data than those of Armstrong-Frederick model, except for trajectory D. However, for 304 steel both models results were far from experimental data, with a maximum difference of 149 MPa (A-F trajectory A), showing the limitation of those models in describing non-proportional behavior.

REFERENCES

ARMSTRONG, P. J., FREDERICK, C. O. (1966). *A mathematical representation of the multiaxial Bauschinger effect*. Report RD/B/N731, CEGB, Central Electricity Generating Board, Berkley, UK.

CHABOCHE, J. L. (1986). *Time-independent Constituive Theories for Cyclic Plasticity*.

CHABOCHE, J. L. (1989). *Constitutive Equations for Cyclic Plasticity and Cyclic Viscoplasticity*.

ITOH, T. (2001) *Multiaxial Low Cycle Fatigue Life Prediction Under Non-Proportional Loading*. Memoirs of the Faculty of Engineering, Fukui University.

JIANG, Y., HERTEL, O.; VORMWALD, M. (2007) *An experimental evaluation of three critical plane multiaxial fatigue criteria*. International Journal of Fatigue, 29, 1490-1502.

SOUZA NETO, E. A.; PERIC, D. E .; OWEN, D. J. D. (2008) *Computational Methods for Plasticity*.